

題名 ISWI Newsletter – Vol. 4 No. 114  
 差出人 George Maeda

---

```
*****
* ISWI Newsletter – Vol. 4 No. 114                      31 October 2012 *
*
*           I S W I = International Space Weather Initiative      *
*                   (www.iswi-secretariat.org)                    *
*
* Publisher:      Professor K. Yumoto, ICSWSE, Kyushu University, Japan *
* Editor-in-Chief: Mr. George Maeda, ICSWSE (maeda[at]serc.kyushu-u.ac.jp)*
* Archive location: www.iswi-secretariat.org (maintained by Bulgaria) *
*           [click on "Publication" tab, then on "Newsletter Archive"] *
* Caveat: Under the Ground Rules of ISWI, if you use any material from *
*           the ISWI Newsletter or Website, however minor it may seem *
*           to you, you must give proper credit to the original source. *
*****
```

Attachment(s):

(1) "Callisto Burst Catalog", 2.5 MB pdf, 10 pages.

```
-----
:           Re:
:           Paper by the PI of the Callisto Project:
:           "Catalog of dynamic electromagnetic spectra
:           observed with Callisto"
:
```

Dear ISWI Participant:

Attached is a fine catalog of various spectra seen by Callisto.

The abstract is thus:

```
: Abstract. This catalog demonstrates dynamic electromagnetic
: spectra observed by Callisto radio spectrometer.
: In the first part natural spectra are presented while in
: the second part we concentrate on artificial (man-made)
: spectra. This catalog shall help the scientist to detect
: and identify weak flares in highly interfered spectra. In
: addition, Callisto spectrometer has proven to be a cheap
: and reliable instrument for radio frequency monitoring.
```

The author of this paper (Christian Monstein) tells me that  
 this paper can also be downloaded from here:

<http://e-callisto.org/papers/BurstCatalog.pdf>

-----> Christian: Excellent work !

Happy Halloween from Fukuoka, Japan,

```
: George Maeda
: The Editor
: ISWI Newsletter
```

# Catalog of dynamic electromagnetic spectra observed with Callisto

Christian Monstein<sup>1</sup>

<sup>1</sup> Institute of Astronomy, ETH Zurich, Switzerland  
e-mail: [monstein@astro.phys.ethz.ch](mailto:monstein@astro.phys.ethz.ch)

Draft 30.04.2011 / Updated 19.06.2011

**Abstract.** This catalog demonstrates dynamic electromagnetic spectra observed by Callisto radio spectrometer. In the first part natural spectra are presented while in the second part we concentrate on artificial (man-made) spectra. This catalog shall help the scientist to detect and identify weak flares in highly interfered spectra. In addition, Callisto spectrometer has proven to be a cheap and reliable instrument for radio frequency monitoring.

**Key words.** Callisto, spectrum, cross modulation, interference, solar flares.

## 1. Introduction

For the convenient interpretation of dynamic solar flare in view of ISWI (International Space Weather Initiative), a catalog of different electromagnetic spectra is presented. Spectra were observed at different locations worldwide and with different antenna systems within the e-Callisto network (Benz, 2004). Observations took place between the years 2004 and 2011. Each figure was built in the same way: wrong channels with high  $\sigma$  eliminated, background subtracted and zoomed to the interesting part.

## 2. Natural spectra

### 2.1. Type I burst (noise storm)

A noise storm consists of long series of short bursts continuing over hours or days. Polarization is always circular and the polarization can change within one day. They are superimpose on a background of slowly varying enhanced radiation which has been described as a "continuum", although it is possible that the background may itself be composed of a large number of overlapping bursts (Menzel, 1960). Noise storms are normally spread over a large frequency band but are rarely seen above 350 MHz. On many occasions the bursts have bandwidths of a few MHz and lifetimes extending from a fraction of a second to nearly 1 minute. At other times bursts of bandwidth nearly 30 MHz and lifetimes less than a second may predominate.

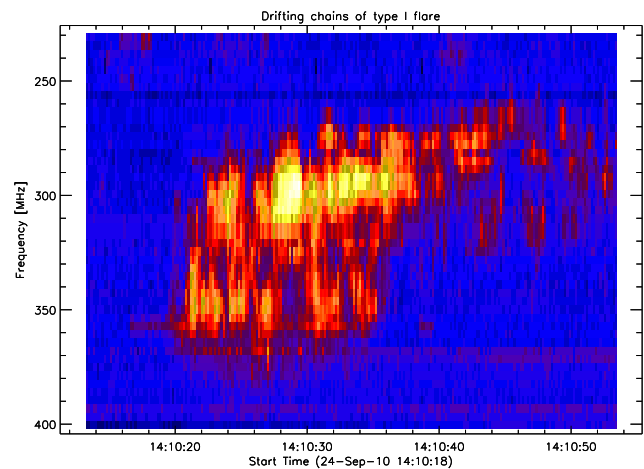


**Fig. 1.** Noise storm or type I solar radio flare observed at Bleien observatory, Switzerland. Antenna = dish 7m, circular polarized.

### 2.2. Type II bursts (slow drift)

A slow drift burst appears as a narrow band of intense radiation which drifts gradually, and sometimes irregularly, toward lower frequencies. Figure 2 shows a typical example. The spectra sometimes show the presence of a second harmonic, but are often so complex as to preclude such identifications. Very often type II burst show a characteristic called 'herring bones' as illustrated in figure 3. The characteristic velocity of the solar disturbance which give rise to these slow burst may be deduced from their rate of change of frequency. This velocity is of the order of 1000 km/sec and as it corresponds to that so-called "auroral corpuscular streams" it has long been held that the slow bursts are caused by the passage of the streams through the solar atmosphere. Alternatively, the bursts may be

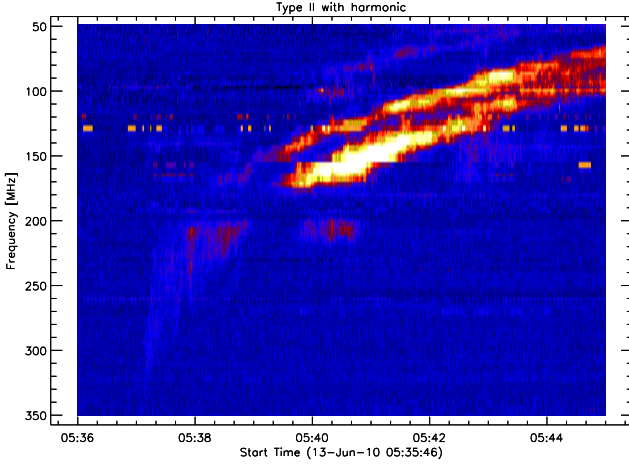


**Fig. 2.** Type II solar radio flare with harmonics observed at Ooty observatory, India. Antenna = logarithmic-periodic linear polarized.

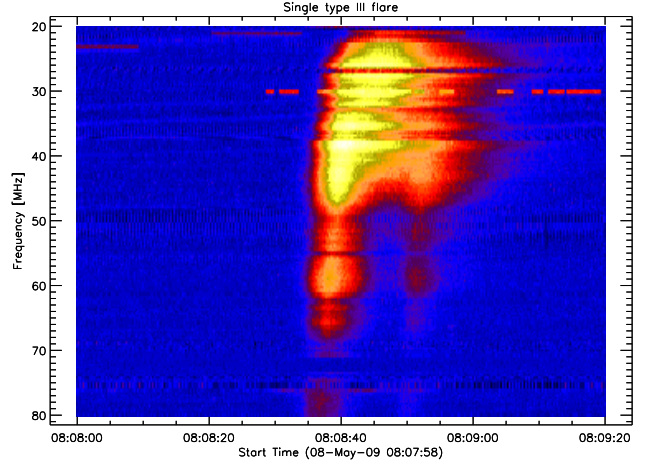


**Fig. 4.** Low frequency isolated type III solar radio flare observed at Bleien observatory, Switzerland. Antenna = logarithmic-periodic CLP-5130.

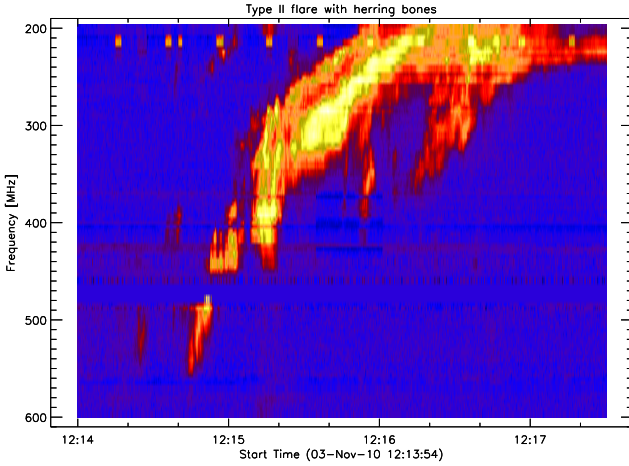


**Fig. 3.** Type II solar radio flare with harmonics and 'herring bones', observed at Bleien observatory, Switzerland. Antenna = parabolic dish 7m, circular polarized.

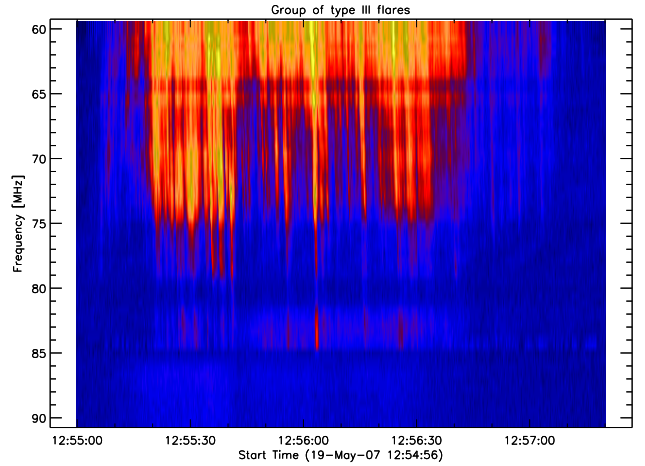


**Fig. 5.** Group of type III solar radio flare observed at Bleien observatory, Switzerland. Antenna = log-per CLP-5130, linearly polarized. Some type III are reverse drifting.

caused by acoustic shock waves resulting from explosions in the lower atmosphere (CME). These waves, being propagated outward at some small multiple of the thermal velocity of the protons, would also be travelling at a velocity of the order of 1000 km/sec.

### 2.3. Type III bursts (fast drift)

Fast drifting bursts, a very commonly occurring phenomenon, have durations of a few seconds and show exceedingly rapid drifts toward lower frequencies. They typically occur in groups of 3 to 10 with a total duration of less than 60 sec, as illustrated in figure 4-6.

### 2.4. Type IV burst

The continuum radiation is a steady enhancement of the background level over a wide band of the spectrum, and

is often associated with noise storms (type I). At times, however, an extremely intense form of continuum radiation is observed covering a frequency band of more than 300 MHz, see figure 7. It often occurs after great outbursts, and may last 10-300 minutes. The wavy, periodic intensity variations in frequency are **not** caused by standing waves in the receiving system, they are given by the structure of the type IV flare. This can be observed and proved by comparing the same flare from different locations (e-Callisto network).

### 2.5. Type V burst

Type V flares are always associated with type III flares and follow them after a few seconds. They have some kind of flag pointing to higher frequencies in front of the flare, see figure 8 near 07:39:30UT. Therefore they can unambiguously identified. The emission is quasi continuous with a

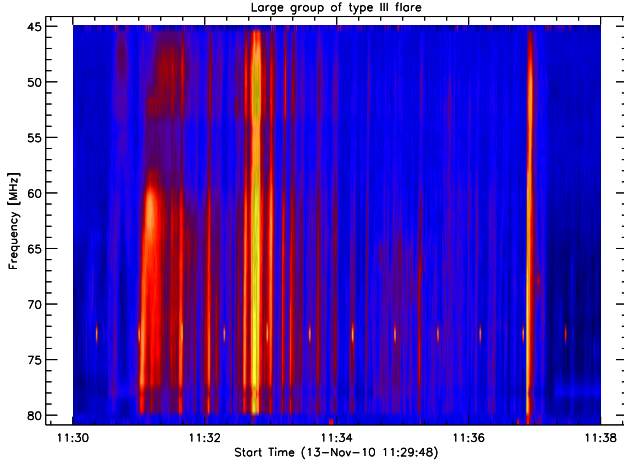


**Fig. 6.** Large group of type III solar radio flare observed at Humain observatory, Belgium. Antenna = log-per CLP-5130, linearly polarized. Probably a U-burst on the left side near 11:31UT.

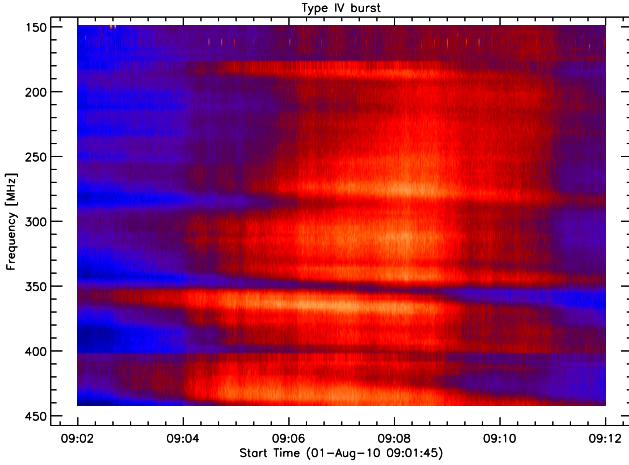


**Fig. 7.** Type IV solar radio flare (continuum) observed in Badary observatory near Irkutsk, Russian Federation. Antenna = log-per CLP-5130, linearly polarized.

bandwidth of less than 200 MHz. Duration is typically less than 1 minute. The emission mechanism is plasma mode transformation (Krüger, 1979) and the exciter are electron streams.

## 2.6. Type DCIM/P burst

Decimetric bursts are quite frequent and cover frequency ranges of many GHz. In figure 9 we can see pulsations in right circular polarisation while at the same time left circular polarization is not pulsed but shows continuum, see figure 10. This needs to be investigated further...

## 2.7. Type DCIM/Z burst

Intermediate drift burst of a DCIM event produced by a X6.9 flare covering hundreds of MHz frequency up

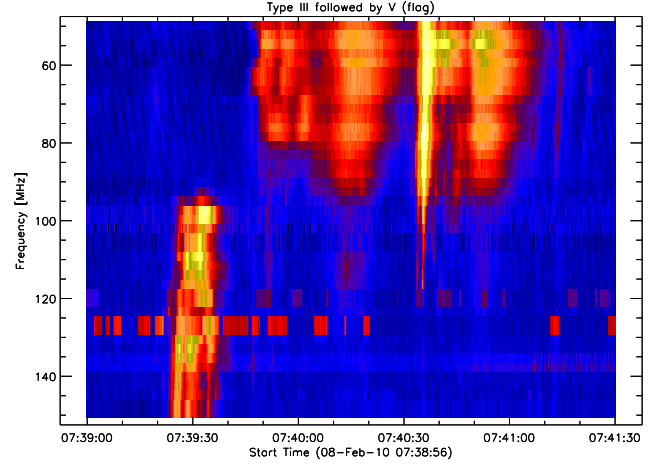


**Fig. 8.** Type V solar radio flare observed at Ooty observatory, India. Antenna = home made, linearly polarized, pointing to zenith.

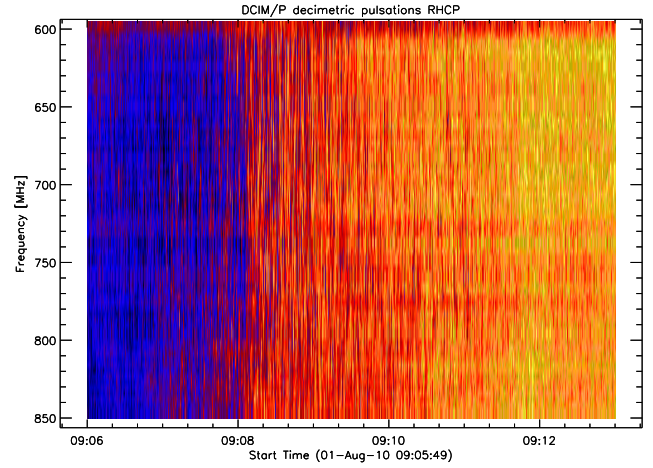


**Fig. 9.** DCIM (decimetric) solar radio flare with pulsations observed at Bleien observatory, Switzerland. Antenna = 7m dish, circularly polarized RHCP, pointing to sun.

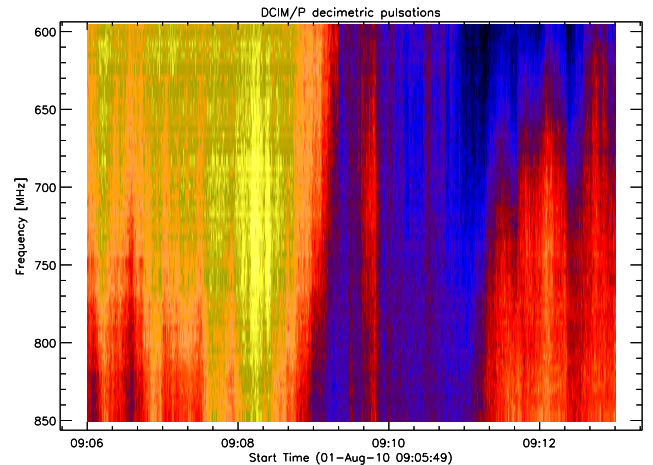


**Fig. 10.** DCIM (decimetric) solar radio flare with continuum observed at Bleien observatory, Switzerland. Antenna = 7m dish, circularly polarized LHCP, pointing to sun.



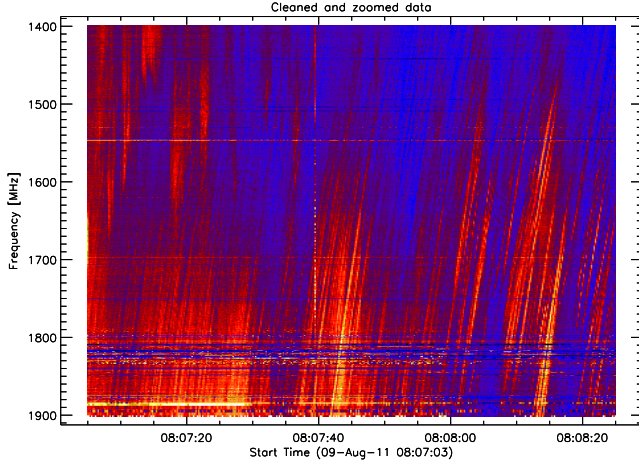


**Fig. 11.** DCIM (decimetric microwave) solar radio flare with zebra structures observed at Bleien observatory, Switzerland. Antenna = 5m dish, pointing to sun.

to 4 GHz. In figure 11 we can see zebra like structures. Therefore also the name zebra-burst. This flare was recorded with Phoenix-3, a FFT-spectrometer.

### 2.8. Synchrotron radiation

Decimetric continuum or synchrotron radiation during active sun produce intensive broad band noise, see figure 12. More frequently in astrophysics, the electrons reach highly relativistic energies. These electrons easily radiate on their own, without any collisions with other particles. They radiate via the cyclotron, synchrotron, and inverse-Compton radiation mechanisms. The cyclotron and synchrotron radiation mechanisms depend on the energy density in magnetic fields. These fields are present everywhere, but they tend to be stronger in those places where electrons are accelerated to high energies, thus helping the high efficiency with which these electrons emit cyclotron or synchrotron radiation

### 2.9. Type U burst

The U-burst, first identified by Maxwell and Swarup and Haddock (Maxwell, 1958), is a type of solar event lasting up to about 10 sec in which the frequency or the emission at first drifts rapidly downwards, then increases again. On the dynamic spectrum record the burst has appearance of an inverted letter U, see figure 13. The frequency drift rate at the sides of the 'U' is of the same order as that observed in ordinary type III bursts; the U-burst is now generally regarded as sub-class of type II, and is believed to be generated by plasma waves set up by fast electron streams in the solar corona

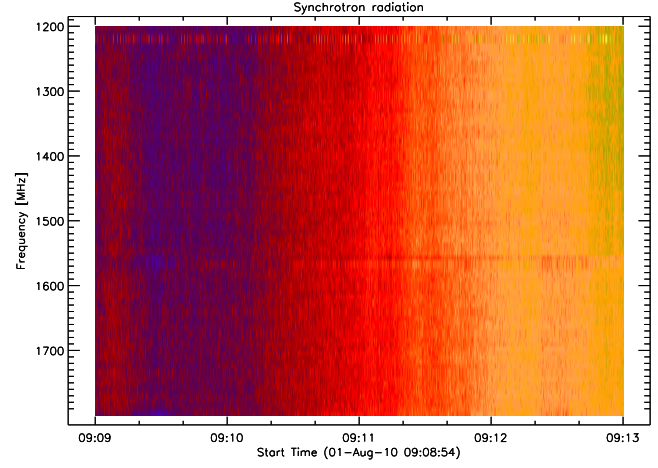


**Fig. 12.** Synchrotron solar radio radiation observed in L-band at Bleien observatory, Switzerland. Antenna = 5m dish, linearly polarized, pointing to sun.

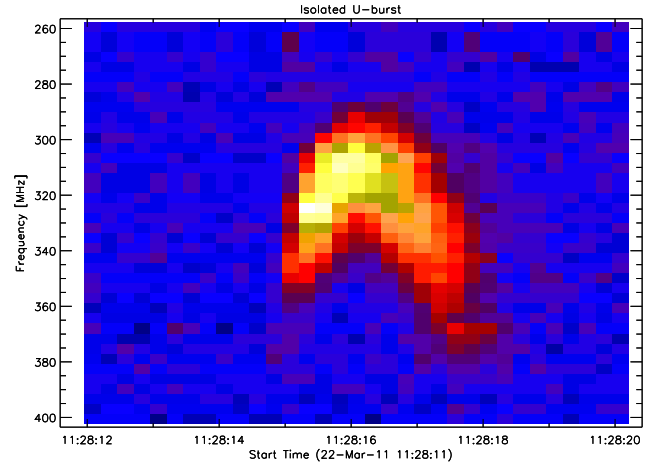


**Fig. 13.** U-burst in intensity (LHCP+RHCP). Antenna = 7m dish, circular polarized, pointing to sun.

### 2.10. Interference from ground reflection

Interference from ground happens only in linear horizontal polarization if the ground is reflective due to water, metal or plants. Also buildings or other large constructions may lead to interference effects. This happens mainly during sun-rise and sun-set when the elevation of the sun is low meaning when the reflected radiation and the direct radiation are both within the beam of the antenna, see figure 14. Detectable interference from solar radiation proves that quiet solar flux of 2s can be measured thus, the system is sensitive down to quiet solar flux.

### 2.11. Terrestrial lightning

During local thunderstorms the telescope receives electromagnetic radiation from lightning strokes. They have similar structure as solar type III bursts, see figure 15. Assuming that these waves were generated by some kind

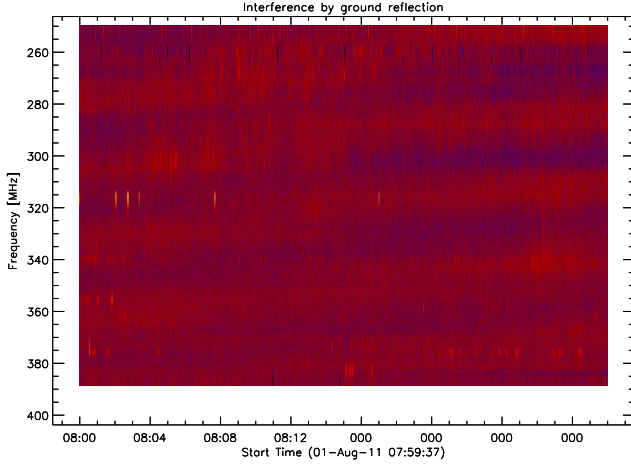


**Fig. 14.** Interference due to reflection of the solar radiation on the ground. Antenna = log-per at station Humain of Royal Observatory of Belgium ROB, linearly polarized, pointing to sunrise.

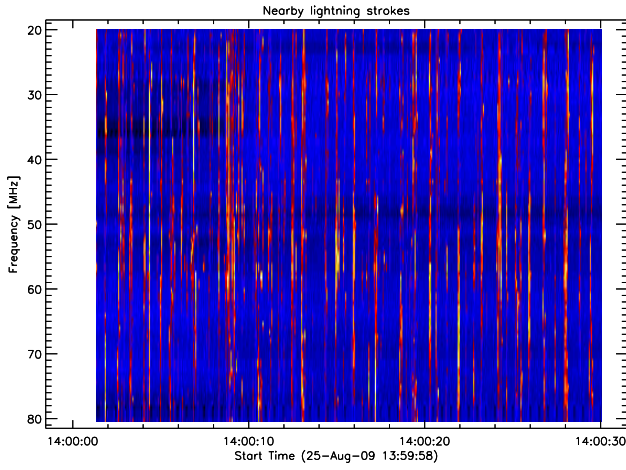


**Fig. 15.** Broad band radiation generated by nearby lightning strokes observed at Bleien observatory, Switzerland. Antenna = biconical dipole, linearly polarized.

of Dirac-pulse the spectrum must be broad band and flat, thus lightning strikes could be used to calibrate standing waves of the telescope.

### 2.12. Microwave pulsations

### 2.13. Transit quiet sun

### 2.14. Calibration steps

## 3. Artificial (man-made) spectra

### 3.1. Electric (Plasma) welding

To the end of August 2004 new rails were installed to secure our scaffold at both telescopes in Bleien. The rails had to be welded together with an electric plasma welding tool. While the welding operator was working, all instruments were operational and we got very strong interference due

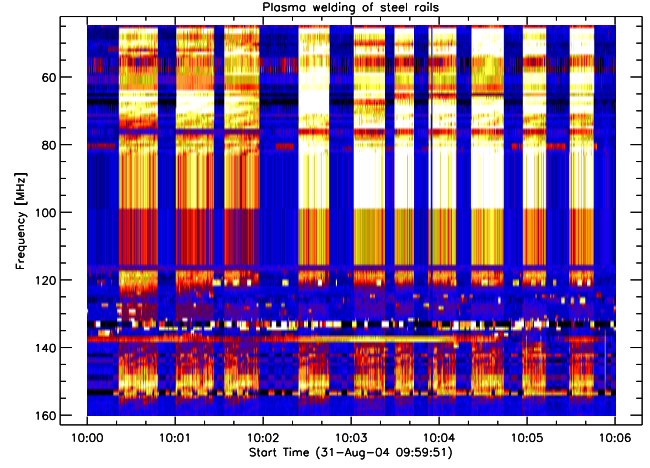


**Fig. 16.** Interference due to manual plasma welding near the telescope observed at Bleien observatory, Switzerland. Antenna = log-per CLP-5130, linearly polarized  $45^\circ$ .

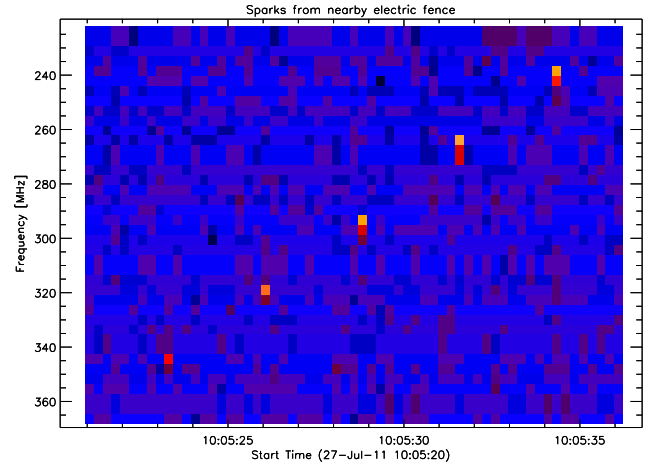


**Fig. 17.** Interference due to electric fence near the telescope observed at Bleien observatory, Switzerland. Antenna = parabolic dish 7m, linearly polarized  $45^\circ$ .

to the electromagnetic fields of the fast changing current in the connecting wiring. Assuming that these interference is broad band one could try to use this pseudo-flare for calibration.

### 3.2. Electric fence

The nearby farmer uses to keep his cows near the telescopes during summer for feeding. To keep the cows in a defined area, an electric fence was installed. The electric fence had a distance of about 5m to the telescopes. Sparks between wire and large blades of grass lead to short and intensive electromagnetic fields producing bright pixels in the spectra, see figure 17. These bright pixels are pseudo-periodic and appear as diagonal structures in the spectrum from bottom left to top right. After discussions with the farmer the electric fence was switched off when no cows were around.

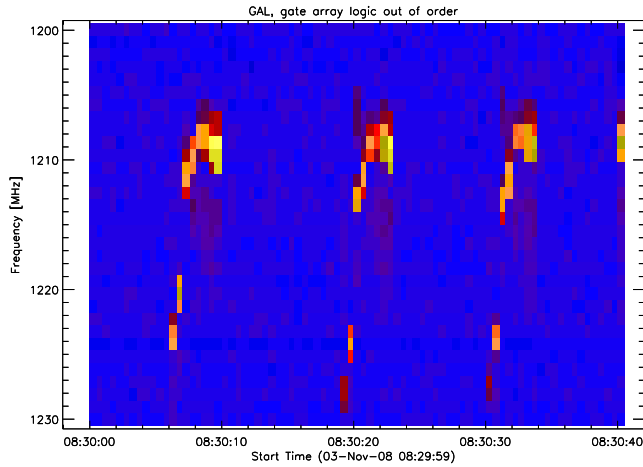


**Fig. 18.** Interference due to damaged gate array logic in the front-end of the telescope observed at Bleien observatory, Switzerland. Antenna = parabolic dish 5m, linearly polarized  $45^\circ$ .

### 3.3. Damaged GAL (gate array logic)

A very time consuming problem occurred in November 2008. Some periodic structure like a U-burst in L-band with a time period of about 15 seconds, see figure 18. Only with some high sophisticated measuring equipment of OFCOM it was possible to identify the source. It was a damaged GAL (gate array logic) in the front-end control board of the 5m dish at Bleien observatory. After replacement of the GAL everything was o.k. again.

### 3.4. Damaged Mini Circuits pre-amplifier

Another very time consuming problem occurred in mid 2011. Some strange, very strong low frequency interference with a time period of about 10 milliseconds appeared on all observed frequencies, see figure 19. After many month of investigation, technicians from MRT found the source of rfi. It was a damaged pre-amplifier from MiniCircuits which started to oscillate after a lightning stroke hit the antenna. After replacement of the pre-amplifier everything was o.k. again.

### 3.5. Interfering LED driver

After installation of a new Callisto spectrometer at Metsähovi observatory we got an extremely high level of interference below 1 GHz, see figure 20. It took more than one month to find out the source of the radiation. It was a simple driver circuit for LED illumination in the observatory. After replacing this non-conform circuit the spectrum was clean and free from interference as one would expect in a protected zone.

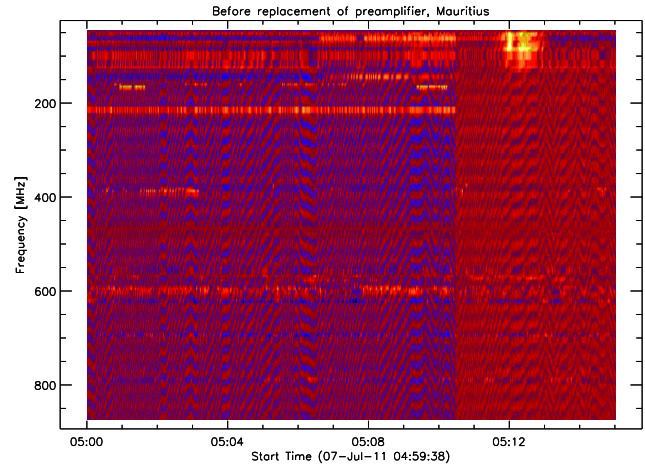


**Fig. 19.** Interference due to damaged pre-amplifier in the front-end of the telescope observed at MRT observatory, Mauritius. Antenna = large log-per, linearly polarized pointing to sky. Type III solar flare top right with about 30 sfu (300'000 Jansky).

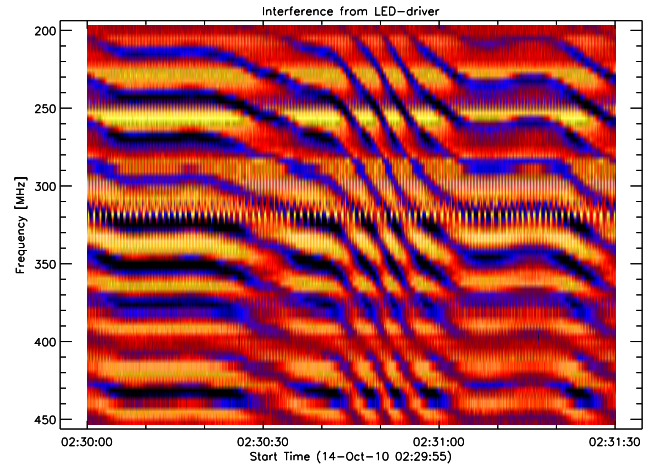


**Fig. 20.** Interference due to LED-driver circuit near the telescope observed at Metsähovi observatory, Finland. Antenna = log-per DVB-T like, linearly polarized.

### 3.6. Doppler shifted transponder of SMART-1

In September 2nd 2006, the ESA satellite SMART-1 was observed during its perilunar orbit before crashing onto the moons surface. The plot shows the doppler shifted down-link signal of the S-band transponder, see figure 21. The observed frequency range at the rf-level was between 2230 MHz and 2239 MHz. The plot shows the down-converted (AR5000) frequency shifted into the audio-range (KHz) of a sound-card FFT-spectrometer.

### 3.7. Electric arc on Pantograph of train

This burst is not a burst at all, it just looks like a solar noise storm or type I burst. In fact it's complete man-made caused by bad electric contact between pantograph of the train and the power line and/or bad contact of the



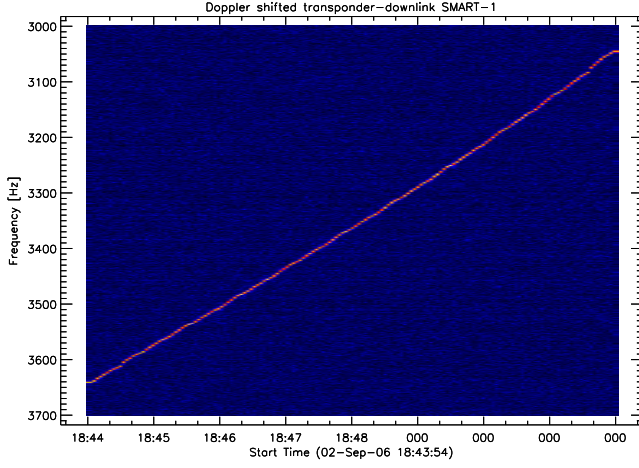


**Fig. 21.** Weak transponder signal from SMART-1 in its per-lunar orbit. Antenna = 5m dish, linearly polarized.

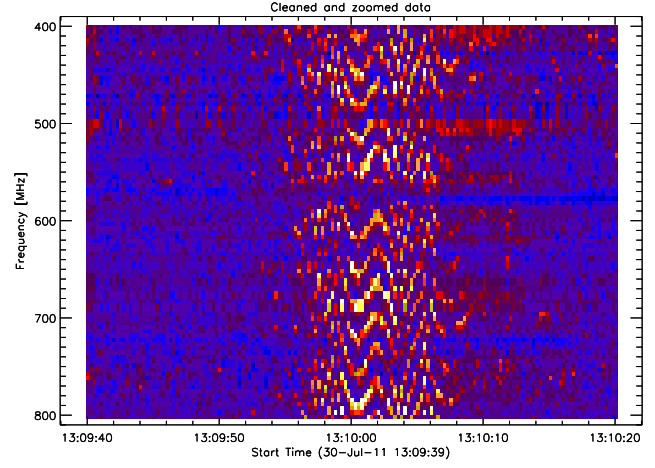


**Fig. 23.** Necklace burst man made by a lawn cutter. Antenna = log-per, linearly polarized.

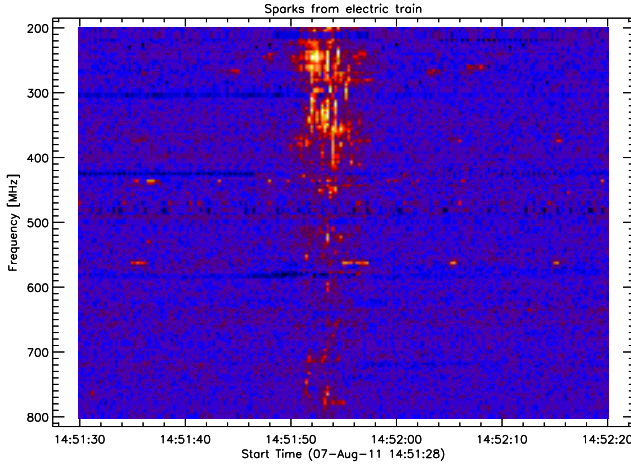


**Fig. 22.** Quasi burst caused by a nearby electric train (SOB). Antenna = log-per, linearly polarized.

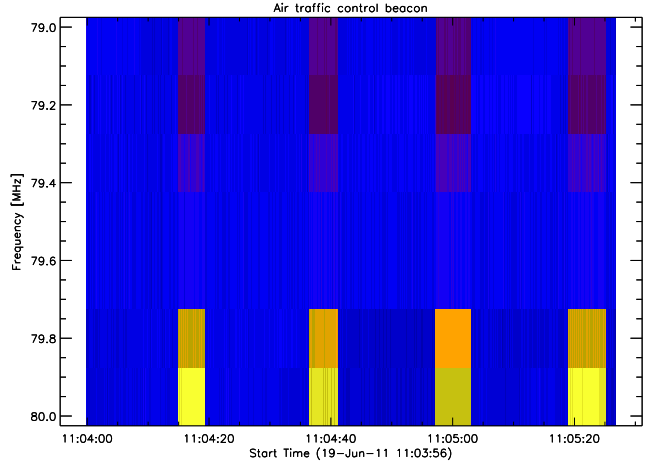


**Fig. 24.** Beacon of local airport used for radio-navigation. Period about 20 seconds with high transmission power.

wheels to the rails. This burst doesn't show any periodic structure.

### 3.8. Lawn cutter 'Necklace' burst

The 'necklace'-burst is not a burst at all, it just looks like a regular pulsating solar burst. In fact it's complete man-made by quasi-periodic interruptions of an electric current. Possible source are lawn cutter, electric drill, motor cycle etc.

### 3.9. Aeronautical radio-navigation beacon 79 MHz

The range 70-80 MHz is mainly reserved for radio-navigation for air-traffic, see figure 24. Very often these signals produce cross-modulation in low-noise/high gain pre-amplifiers.

### 3.10. FM radio 87.5-108 MHz

The FM-band is fully occupied with local transmitters leading to high noise level on all channels in the band, see figure 25. In many radio-telescopes this band has to be notched with a band-stop filter (FM-trap). Callisto software allows to 'jump' over the whole band and to ignore these channels.

### 3.11. Aeronautical communication 117-137 MHz

The aeronautical band is sporadically occupied but 24h/day, see figure 26. The modulation is still AM (amplitude modulation) and may lead to saturation if the aeroplane is directly in sight of the antenna.

### 3.12. Radio amateur communication 144-146 MHz

HAM or radio amateurs have access to their own bands and use it for 24h/day, see figure 27. The power level is



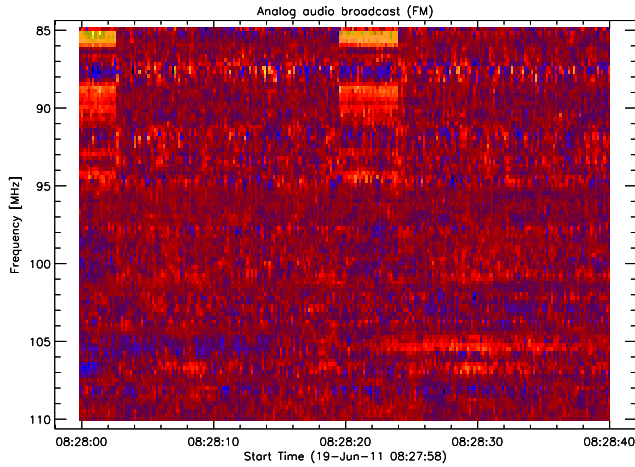


**Fig. 25.** FM (frequency modulation) band with full occupation of the band. All channels are nearly saturated.

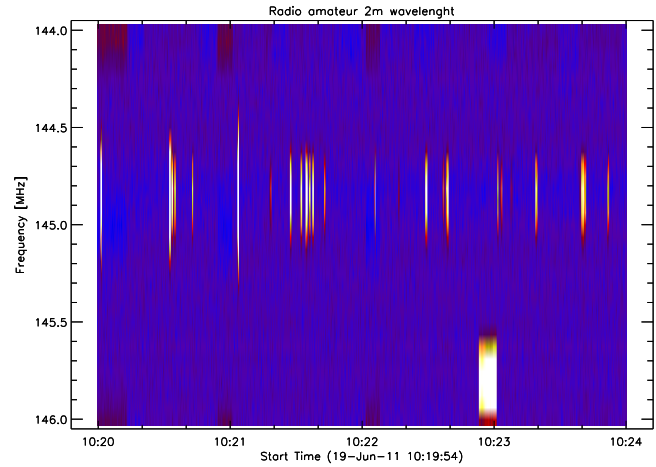


**Fig. 27.** Sporadic NFM (narrow frequency modulation) from amateur radio communication (HAM) in 2m band.

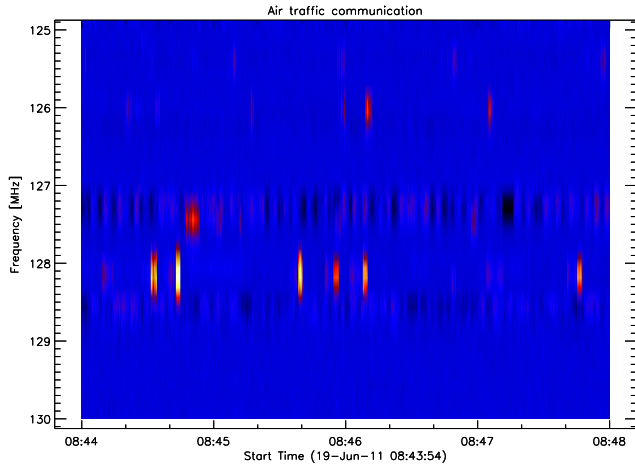


**Fig. 26.** Sporadic AM (amplitude modulation) from air traffic communication.

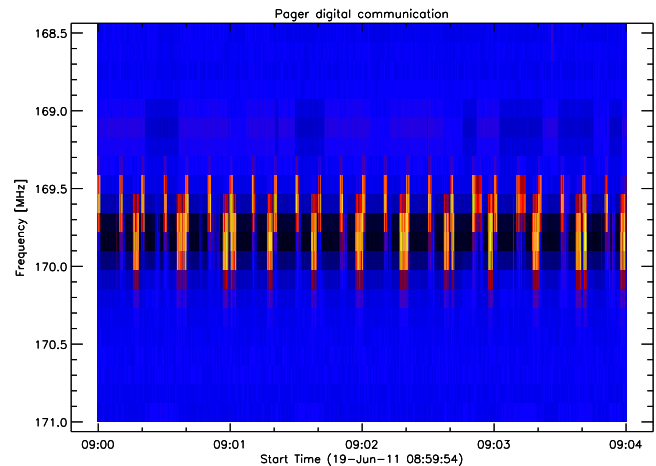


**Fig. 28.** Permanent communication in NFM-FSK (narrow band frequency frequency shift keying).

limited, therefore interference is limited to telescopes with nearby operators. The same range is also reserved for amateur satellites.

### 3.13. Pager and tracking system 169.4-169.825 MHz

Permanent communication 24h/7d in NFM-FSK (narrow band frequency frequency shift keying, see figure 28). These types of signal have strong influence to high gain pre-amplifiers and very often lead to saturation or cross-modulation. Some low frequency radio-telescopes need a notch-filter to suppress these signals.

### 3.14. DAB-T 216-230 MHz

Digital terrestrial sound or television broadcast 24h/7d with high power and sharp edges in frequency range, see figure 29. Sometimes a phase locked structure can be recognized in the spectrum. Astronomical observations within DAB-channels are not possible.

### 3.15. Stationary (military) satellites 235-310 MHz

Many military satellites (MILSATCOM, UFO Follow On etc.) in geostationary position have down-link transponders in VHF-range, see figure 30. They are rather strong but there are always channels which are free and can therefore be used for observations. These transponders signals are very convenient for a quick check of the radio telescope. Under normal condition (antenna=log-per, low noise pre-amplifier without cooling) leads to a Y-factor of about 10 dB. This is the case for linear polarization, although the transponder are left circular polarized.

### 3.16. TETRA 380-395 MHz

(TERrestrial Trunked Radio) is an international standard for digital mobile communications. TETRA systems are gradually being adopted in European countries by police forces and other emergency services. TETRA bears some resemblance to the digital mobile phone networks, but

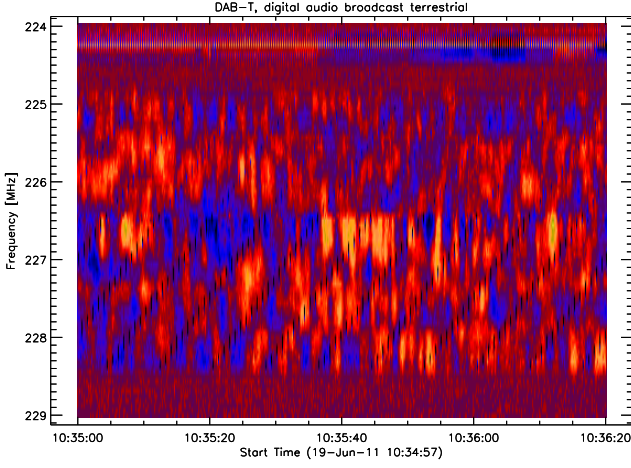


**Fig. 29.** Permanent (24h/7d) communication in DAB-T (digital audio broadcast terrestrial).

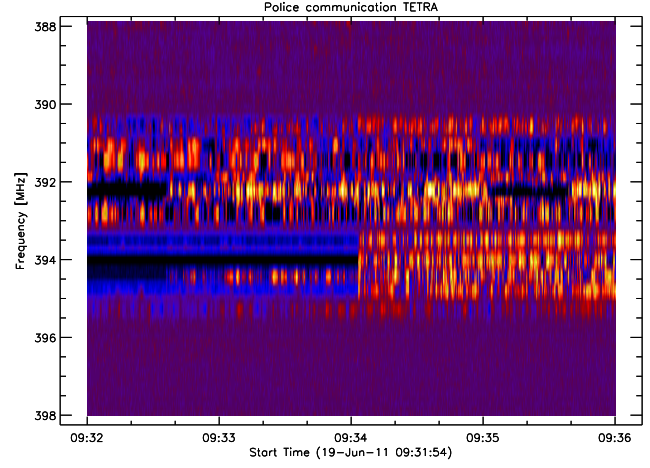


**Fig. 31.** TETRA, permanent communication 24h/7d in digital broad-band transmission.

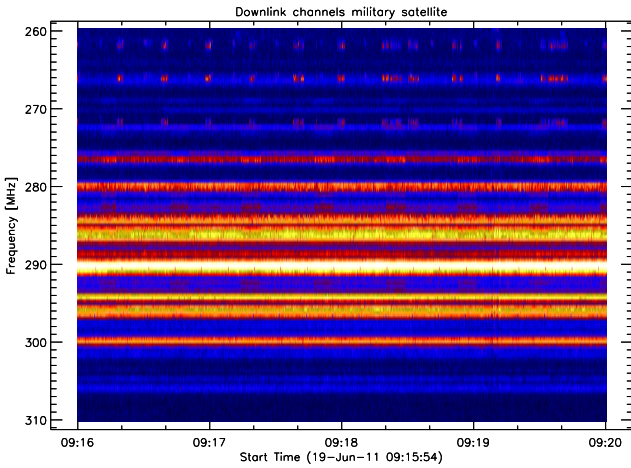


**Fig. 30.** Permanent (24h/7d) communication of military satellites.

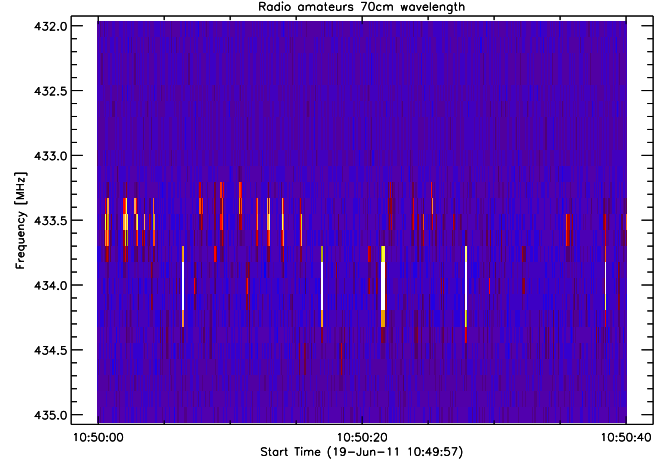


**Fig. 32.** Sporadic NFM (narrow frequency modulation) from amateur radio communication (HAM) in 70cm band.

generally the cells are larger and the transmission powers higher. The introduction of any new transmission system is likely to cause some degree of interference to existing services, see figure 31. The problems caused to Radio-Astronomy and TV reception by TETRA, however, seem to be much more widespread than anyone anticipated. There are deep political issues involved with the implementation of TETRA. The frequencies allocated for police and fire service TETRA use are 380 - 385 MHz (mobile) and 390 - 395 MHz (fixed).

### 3.17. Radio amateur communication 430-438 MHz

Shared 70 cm band mainly used by radio amateurs (HAM-operators) for communication, including amateur satellites. The power level is limited, therefore interference is limited to telescope sites with nearby operators. In the same band we can also see quasi periodic communication from remote (temperature) sensors, see figure 32.

### 3.18. DVB-T 470-608 MHz

DVB-T stands for terrestrial digital television broadcast and multi-media services. The spectrum shows very sharp edges at the border of the spectrum. In the band there is no chance for any radio-astronomical observations. The power level is very high without any structure in the spectrum, see figure 33. If zooming into the spectrum, it looks like a solar noise storm.

### 3.19. SRD 862-870 MHz

In telecommunication, a low-power communication device, also short-range device (SRD) is a restricted radiation device, exclusive of those employing conducted or guided radio frequency techniques, used for the transmission of signs, signals (including control signals), writing, images and sounds or intelligence of any nature by radiation of electromagnetic energy. Examples: Wireless microphone, phonograph oscillator, radio-controlled garage

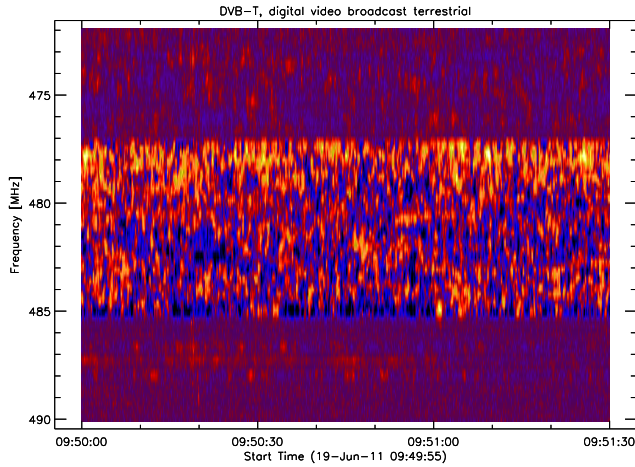


**Fig. 33.** DVB-T (digital video broadcast terrestrial, a permanent transmission in broad band technology.

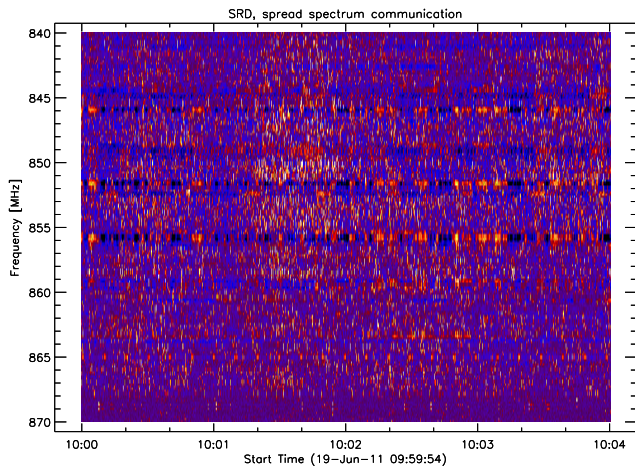


**Fig. 34.** SRD (short range device) band as broad band digital transmission 24h/7d looking like solar decimetric pulsations.

door opener, and radio-controlled models. Low Power Device 433 MHz (LPD433) transceiver radios are short range, licence free communication devices used throughout the world. They operate in the UHF band from 433.075 MHz to 434.775 MHz with 25 kHz channel spacing, for a total of 69 channels. These devices are frequency modulated (FM) with a maximum legal power output of 10 mW. LPD devices must only be used with the integral and non-removable antenna. LPD was introduced to reduce the burden on the eight PMR446 channels over shorter ranges (less than 1 km). Channels 1 to 14 are UK Amateur repeater outputs and channels 62 to 69 are UK Amateur repeater inputs. European licence-free LPD transceivers also include Short Range Device 860 MHz (SRD860), which have a maximum legal power output of 5 mW, see figure 34. SRD has a total of 126 channels in five bands. This kind of transmission can easily be mixed up with decimetric pulsations of solar bursts.

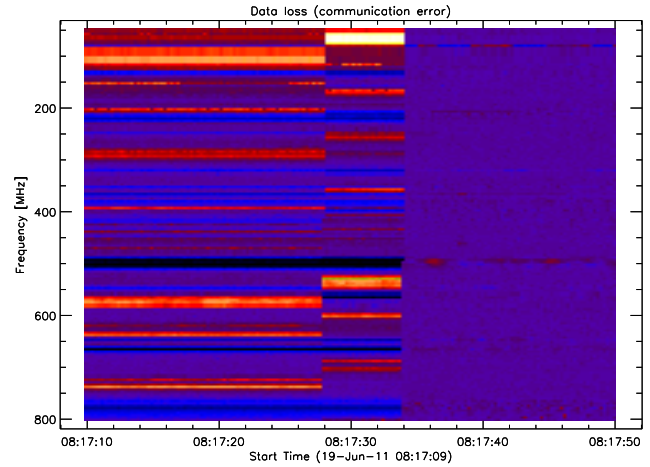


**Fig. 35.** Twice data loss near 08:17:30UT due to inappropriate resources of an old PC.

### 3.20. Data loss

Data loss can happen due to inappropriate resource of the control-PC, see figure 35. Main reasons are:

1. bad quality of the RS-232 cable or a too long cable.
2. bad quality of RS-232/USB converter
3. bad selection of interrupt level
4. not enough working memory (RAM)
5. too many applications running on the PC
6. PC with insufficient resources

The effect is, that the spectrum jumps in frequency. In this case all channels are wrong.

### 3.21. Non-stationary satellite

### 3.22. Unstable antenna positioning

### 3.23. Rain changing antenna parameter

### 3.24. Temperature change receiver

### 3.25. Weather monitor, remote sensor

### 3.26. Saturation

## 4. Unknown spectral sources

### References

- Donald H. Menzel *The Radio Noise Spectrum*, Haward University Press, Cambridge, Massachusetts, 1960.
- Albrecht Krüger *Introduction to Solar Radio Astronomy and Radio Physics*, D. Reidel Publishing Company, Dordrecht, 1979.
- Arnold O. Benz, Christian Monstein and Hansueli Meyer *CALLISTO, A New Concept for Solar Radio Spectrometers*, Kluwer Academic Publishers, The Netherlands, 2004.
- Maxwell A. and Swarup G. *A new spectral characteristic in solar radio emission*, Nature 181, 36 - 38 (04 January 1958), 1958.